Computational and Structural Biotechnology Journal 20 (2022) 5966–5977

COMPUTATIONAL ANDSTRUCTURAL BIOTECHNOLOGY JOURNAL

journal homepage: www.elsevier.com/locate/csbj

Quantitative proteomic analysis reveals the molecular mechanism of the Yesso scallop (*Patinopecten yessoensis*) in response to *Polydora* infection

Hongyan Sun, Junxia Mao *, Yiying Wang, Zhiyue Fan, Changzi Yuan, Xubo Wang, Ying Tian, Bing Han, Zhenlin Hao, Jun Ding, Yaqing Chang *

Key Laboratory of Mariculture & Stock Enhancement in North China's Sea, Ministry of Agriculture and Rural Affairs, Dalian Ocean University, Dalian, China

ARTICLE INFO

Article history:
Received 8 June 2022
Received in revised form 20 October 2022
Accepted 27 October 2022
Available online 2 November 2022

Keywords:
Yesso scallop
Polydora
Mantle
Proteomics
Response mechanism

ABSTRACT

The Yesso scallop is a large and ancient molluscan group with great economic value; however, it has recently suffered severe cases of *Polydora* infection. *Polydora* parasitizes the shells of scallops, badly damaging shell structures and affecting growth and mortality. To investigate the molecular mechanism of Yesso scallops' response to *Polydora* infection, proteomic profiling changes in the mantle tissues of *Polydora*-infected (diseased) and healthy scallops were systematically analysed by tandem mass tags (TMT) labelling technology in this study. A total of 519 differentially expressed proteins (DEPs) were identified. Gene Ontology (GO) and Kyoto Encyclopedia of Genes and Genomes (KEGG) analysis revealed most innated immune-related functions and pathways were significantly downregulated in diseased scallops, except the phagocytosis pathway, indicating an important role of phagocytosis in response to *Polydora* infection. DEPs involved in the phagocytosis pathway were associated with phagocytic receptor recognition, phagosome biogenesis and pathogen degradation, and they were further verified by quantitative real-time PCR. The results elucidate the molecular components of phagocytosis in molluscs for the first time. *Polydora* can be encapsulated by melanization with an obvious appearance in shells; indeed, melanization-related DEPs were upregulated in diseased scallops. Inhibition of apoptosis and nervous modulation may be also involved in the response mechanism, with some highly associated proteins significantly differentially expressed. Finally, a protein–protein interaction network was constructed to provide a global view of the interaction relationships of the DEPs. The study predicts the molecular response mechanism of Yesso scallops to *Polydora* infection, and lays a theoretical foundation for *Polydora* disease control.

1. Introduction

The Yesso scallop (*Patinopecten yessoensis*) is a large and ancient molluscan group endemic to the coastlines of northern Japan, far eastern of Russia and the northern Korean Peninsula [1]. Due to its high economic value, the Yesso scallop has become a major economic aquaculture species in Asian countries and is consumed worldwide [2]. Recently, frequent disease outbreaks associated with *Polydora* infection have strongly impacted the growth and quality of many bottom-sown shellfishes, including the Yesso scallop, causing great economic losses [3–5]. *Polydora* mainly parasitize the left shell of the scallop (as shown in Fig. 1) by excavating tunnels in it via the chemical secretion of acidic mucus and mechanical friction, which badly damages the shell structure [6–8]. As a result, melanization is found on the inner surface of the affected shell. When serious, *Polydora* will drill through the shell, directly infect the soft body, and expose the scallop to various pathogens. The molecular response mechanism of the Yesso scallop to *Polydora* infection is probably very complex, being associated with biomineralization and immunomodulation. However, related research is very scarce, which limits our understanding of the immune mechanisms of scallops and the exploration for effective methods of *Polydora* disease control.

Like all invertebrates, scallops are generally considered as lacking a complex adaptive immune system. To resist invaders, they rely solely on innate immunity mediated by cellular and humoral components [9]. The mantle tissue, an evolutionary homologous organ in molluscs, is located midway between the shell and visceral mass. It supports production of the shell, which provides the first line of physical defence [10]. This tissue is mainly

* Corresponding authors.
E-mail addresses: maojunxia@dlou.edu.cn (J. Mao), changlab@hotmail.com (Y. Chang).

https://doi.org/10.1016/j.csbj.2022.10.043

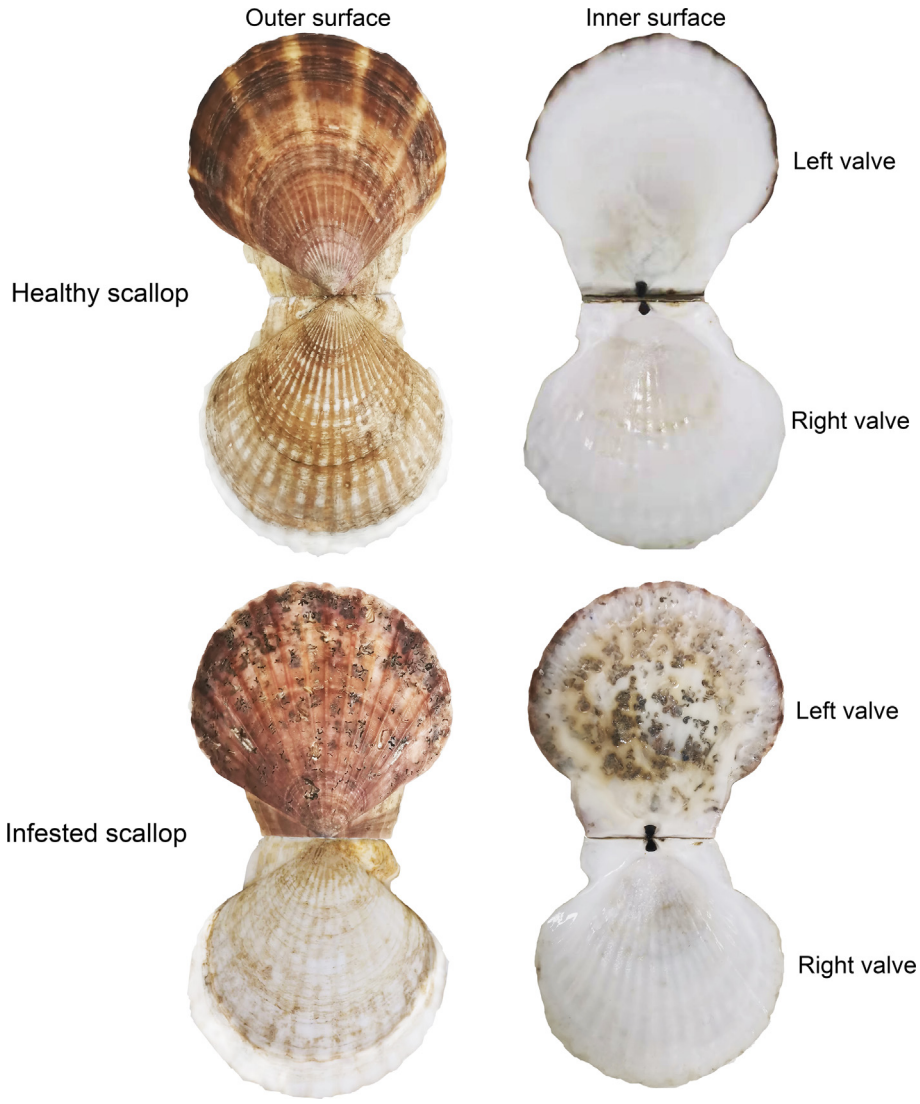

Fig. 1. Shell surface features of the healthy and *Polydora*-infected Yesso scallops. *Polydora* mainly parasitizes the left shell by excavating tunnels, while melanization is found on the inner surface.

constituted by two simple epithelial layers separated by connective tissue. There are rich mucous cells distributed among the epithelia that play important roles in shell matrix secretion and mucosal immunity [10–13]. Components of mucosal immunity in molluscs are involved in pathogen recognition, immune activation, cell signalling and immune effectors [13]. Besides, these mucosal epithelia can also have phagocytic activity, which contributes to microbial homeostasis and limits infections [13]. Our previous histological study found that *Polydora*-infected Yesso scallops had significantly more mucous cells in the epithelia of their mantle tissues than healthy individuals. This indicates the key roles of these cells in response to *Polydora* infection [14]; however, the underlying molecular mechanism remains largely unclear.

In recent years, proteomics has become an essential technique for exploring molecular mechanisms of disease resistance in plants and animals, as it allows for the analysis of expression profiling changes in cell or tissue proteins and provides information about protein regulation and active pathways [15–17]. Most previous proteomic studies in marine invertebrates relied upon two-dimensional gel electrophoresis, which is limited by its low throughput and low reproducibility [18–20]. The new proteomics platform, tandem mass tags (TMT) labelling technology, provides more sensitive and reliable measurements for protein identification and quantification with high throughput, and allows simultaneous comparisons of protein profiles in multiple samples [21]. The genome of the Yesso scallop has recently been sequenced and annotated in high quality [22], providing ample information for proteomics analysis of the species.

Based on the characteristics of *Polydora* infection and the obvious histological changes occurring in the mantle tissues of infected Yesso scallops, the present study analysed proteomic profiling changes in the mantle tissues of infected Yesso scallops by TMT labelling technology. The aim was to explore the molecular mechanism of scallops in response to *Polydora* shell infection. Proteins expressing in the mantle tissue were identified, and differentially expressed proteins (DEPs) between diseased and healthy scallops were screened. The functions of the DEPs were elucidated by Gene Ontology (GO) and Kyoto Encyclopedia of Genes and Genomes (KEGG) enrichment analysis, and key molecular pathways involved in response to *Polydora* infection were predicted. Further, the expression levels of genes involved in key pathways were verified by quantitative real-time PCR (qRT-PCR). Finally, protein–protein interactions (PPi) were analysed to obtain a global view of the interaction relationships of the DEPs. The study predicts the molec-

ular mechanism of the Yesso scallop in response to *Polydora* infection, which will help us to better comprehend the innate immune mechanisms of molluscs and lay a significant theoretical foundation for *Polydora* disease control.

2. Materials and methods

2.1. Scallop collection

Two-year-old healthy and *Polydora* infected Yesso scallops (Fig. 1) with an average shell size (shell height) of 10.733 ± 0.665 cm were collected from Dalian Zhangzidao sea area (Liaoning, China). The two groups of Yesso scallops were temporarily acclimated in the laboratory for one week with filtered and aerated seawater at approximately 8 ℃, which is within the optimum temperature range for scallop growth. The mantle tissues of the left valves were sampled and immediately frozen in liquid nitrogen and stored in a –80 ℃ freezer. From the diseased group, individuals were sampled that had most of the area of their left valves infected by *Polydora* (like in Fig. 1). Three biological replicates of each group were prepared for the proteomic experiments. Protein regulation in the mantle tissues of the above diseased and healthy Yesso scallops were characterized and compared.

No specific permits were needed for the described field studies. All the scallops were commercially available cultured marine species and were not endangered or protected species. All experiments were conducted in accordance with the regulations of the local and central governments.

2.2. Protein isolation

The mantle tissues were individually milled to powder in a mortar with liquid nitrogen, then transferred into low-protein binding tubes. Some 600 μL of extraction buffer (0.7 M sucrose; 0.1 M NaCl; 0.01 M dithiothreitol, DTT; 0.04 M EDTA·2Na; 0.125 M Tris-HCl pH 6.8; 0.125 M Tris-HCl pH 8.8) supplemented with 1 mM phenylmethanesulfonyl fluoride (PMSF) were added to each sample. Samples were further lysed by sonication at 80 W for 3 min at 1 s/1s intervals. The same volume of Tris-phenol (pH 7.8) was added and mixed for 30 min at 4 °C. Furthermore, the mixtures were centrifuged at 7100*g* for 10 min at 4 °C to collect phenol supernatants. The supernatants were added to 5-times volumes of 0.1 M cold ammonium acetate–methanol buffer and precipitated at –20 °C overnight. After precipitation, the samples were centrifuged at 12,000*g* for 10 min to collect the precipitate. Then, the precipitate was washed with 5-times volumes of cold methanol and gently mixed. The precipitate was centrifuged at 12,000*g* for 10 min at 4 °C again to collect washed precipitate, and this process repeated once more. Then, methanol was replaced by acetone and the wash process repeated twice more to remove methanol contamination. The samples were centrifuged at 12,000*g* for 10 min at 4 °C to collect the final precipitate, which was dried at room temperature for 5 min and dissolved in lysis buffer (1 % sodium dodecyl sulfate, SDS) for 3 h. Finally, the samples were centrifuged at 12,000*g* for 10 min and the supernatant were collected. The supernatant samples were centrifuged again to remove the precipitate completely. Protein concentrations were determined using a BCA kit (Thermo Fisher Scientific).

2.3. Protein digestion and TMT labelling

Some 100 μg protein of each sample was added to DTT to a final concentration of 4.5 mM and incubated at 55 °C for 30 min. After cooling on ice to room temperature, iodoacetamide was added to the solution to a final concentration of 9 mM in darkness at room temperature. After 15 min, six volumes of cold acetone were added and the solution was precipitated at –20 °C overnight. The samples were centrifuged at 8000 g for 10 min at 4 °C collect the precipitate. The precipitate was dissolved with 100 μL 300 mM tetraethyl ammonium bromide (TEAB), followed by 2 μg sequencing-grade trypsin, then the solutions were incubated for digestion at 37 °C overnight.

For TMT labelling, the lyophilized samples were resuspended in 100 μL 200 mM TEAB and 30 μL of each sample was transferred into a new tube for labelling. Some 41 μL of TMT label reagent from a TMT10plex™ kit (Thermo Fisher Scientific) was added to each sample for mixing (3 healthy scallops: C1-126 label, C2-127N label, C3-127C label; 3 diseased scallops: D1-129C label, D2-130N label, D3-130C label; mix: 131 label). The tubes were incubated at room temperature for 1 h. Finally, 8 μL of 5 % hydroxylamine was added to each sample and incubated for 15 min to quench the reaction. The labelling peptides solutions were lyophilized and stored at –80 °C.

2.4. Reversed-phase liquid chromatography (RPLC) fractionation

Reversed-phase (RP) separation was performed on an 1100 high-performance liquid chromatography (HPLC) system (Agilent) using an Agilent Zorbax Extend RP column (5 μm, 150 mm × 2.1 mm). Mobile phases A (2 % acetonitrile in HPLC water) and B (90 % acetonitrile in HPLC water) were used for RP gradient. The solvent gradient was set as follows: 0–8 min, 98 % A; 8–8.01 min, 98 %–95 % A; 8.01–48 min, 95 %–75 % A; 48–60 min, 75–60 % A; 60–60.01 min, 60–10 % A; 60.01–70 min, 10 % A; 70–70.01 min, 10–98 % A; 70.01–75 min, 98 % A. Tryptic peptides were separated at a fluent flow rate of 300 μL/min and monitored at 210 nm and 280 nm. Samples were collected for 8–60 min, and eluent was collected in centrifugal tubes 1–15 every minute in turn. Samples were recycled in this order until the end of gradient. The separated peptides were lyophilized for mass spectrometry.

2.5. LC-MS/MS analysis

All analyses were performed by a Q-Exactive HF mass spectrometer (Thermo) equipped with a Nanospray Flex source (Thermo). Samples were loaded and separated by a C18 column (15 cm × 75 μm) on an EASY-nLCTM 1200 system (Thermo). The flow rate was 300 nL/min and linear gradient was 60 min (0–1 min, 2–9 %B; 1–45 min, 9–29 % B; 45–52 min, 29–37 % B; 52–56 min, 37–100 % B; 56–60 min, 100 %B; mobile phase A = 0.1 % FA in water and B = 0.1 % FA in ACN). Full MS scans were acquired in the mass range of 350–1500 m/z with a mass resolution of 60,000, and the AGC target value was set at 3e6. The 10 most intense peaks in MS were fragmented with higher-energy collisional dissociation (HCD) at a collision energy of 32 MS/MS. Spectra were obtained with a resolution of 45,000 with an AGC target of 2e5 and a maximum injection time of 80 ms. The Q-Exactive HF dynamic exclusion was set for 30 s and run under positive mode.

2.6. Database search and bioinformatics analysis

ProteomeDiscoverer (version 2.4) was used to search all of the raw data thoroughly against the protein database derived from the annotation of the Yesso scallop genome [22]. The database search was performed with trypsin digestion specificity, and carbamidomethyl on cysteine was considered as fixed modifications. The TMT 10 plex labeling method was selected for protein quantification. Screening of proteins was performed using the parameters of peptide ≥2 and false discovery rate (FDR) <1 %. Differentially expressed proteins (DEPs) were identified with *t*-tests. Proteins with a Foldchange ≥1.2 or ≤0.83 and $p < 0.05$ were considered

to be differentially expressed between diseased and healthy Yesso scallops. GO (https://www.geneontology.org) and KEGG (https://www.genome.jp/kegg/) enrichment analysis was employed to analyse the functions of the DEPs. GO enrichment analysis was performed for three ontologies (biological process, molecular function, and cellular component). The GO term or pathway was regarded as a significant enrichment with a threshold of protein number ≥2 and $p \leq 0.05$. Protein-protein interaction (PPi) analysis was based on the String (https://string.embl.de/) database and Cytoscape (https://www.cytoscape.org/) software.

2.7. Quantitative real-time PCR analysis

qRT-PCR analysis for genes involved in phagocytosis was performed following the method mentioned in [23]. Briefly, total RNA was extracted with an RNAprep pure tissue kit (Tiangen) and first-strand cDNA was synthesized using the PrimeScript RT reagent kit (TaKaRa) following the manufacturer's protocols. qRT-PCR was conducted using the FastStart Essential DNA Green Master kit (Roche) on a Roche Light Cycler 96 System (Roche) The running program was as follows: 95 °C for 10 min, followed by 40 cycles at 95 °C for 10 s and 60 °C for 30 s, then 95 °C for 10 s and 65 °C for 1 min and, finally, 97 °C for 1 s and 37 °C for 30 s. Primer Premier 5.0 software was used to design the primers for qRT-PCR, and the primer sequences and product lengths are listed in Supplementary Table S1. The *β-actin* gene was selected as a reference gene [24]. The specificity of the primers was assessed by alignment with the Yesso scallop genome by BLASTN with an e-value of 1e-10. Melting curve analysis was also performed to verify that each primer set amplified a single product. Three technical replicates for each reaction and three biological replicates for each group were used.

Data from the qRT-PCR was processed using the $2^{-\Delta\Delta CT}$ method [25] to assess the relative expression levels of the above genes in the diseased and healthy Yesso scallops. SPSS software (version 22.0) was used to perform independent *t*-tests, and *p* values ≤0.05 were considered statistically significant.

3. Results

3.1. Protein identification and quantification

The protein abundance of the mantle tissues of healthy and diseased Yesso scallops were analysed by the TMT-based proteomics approach. A total of 5177 proteins were identified. The molecular weight distribution of the proteome is shown in Supplementary Fig. S1A, and was mainly concentrated in the range of 0–250 kDa. The distribution of peptide numbers in each protein was shown in Fig. S1B, and the rate of peptide coverage is presented in Fig. S1C. Principal component analysis (PCA) of the protein expression levels shows that samples from the same group were spatially clustered (Fig. 2A), which indicates clear differences between the protein expressions of the diseased and healthy groups. Pearson correlation coefficients among the samples from the same group were high (healthy group: 0.67–0.83, diseased group: 0.78–0.88) and were low among samples from different groups (−0.097–0.025; Fig. 2B), which indicates good reproducibility of the duplicate samples from the two groups.

3.2. Differentially expressed proteins between diseased and healthy Yesso scallops

A total of 519 proteins were identified as being differentially expressed between diseased and healthy Yesso scallops, with a threshold of $p \leq 0.05$ and Foldchange ≥1.2 or ≤0.83 (Table S2). In diseased scallops, 202 proteins were significantly upregulated and 317 proteins were significantly downregulated (Fig. 3A). Volcano plots of the 519 DEPs are shown in Fig. 3B, and hierarchical clustering analysis based on differences in protein expression recovered a clear distinction between the diseased and healthy Yesso scallops (Fig. 3C). Among these DEPs, proteins related to melanization, the innate immune response, apoptosis and the nervous system were identified (Table 1).

3.3. GO functional classification of DEPs

GO enrichment analysis was performed to analyse the functions of the DEPs. A total of 338 GO terms were significantly enriched with a threshold of protein number ≥2 and $p \leq 0.05$, which were further divided into three classes: biological process (BP, 211 terms), cellular component (CC, 52 terms) and molecular function (MF, 75 terms; Table S3). The enriched GO at level 2 for upregulated and downregulated DEPs are shown in Fig. 4, which covers many functions. In BP, most DEPs were enriched in 'cellular process' (70.7 %, 75.3 %), 'metabolic process' (51.0 %, 58.6 %) and 'biological regulation' (38.9 %, 53.6 %). It was noteworthy that 'immune system process' (5.10 %, 20.9 %) and 'response to stimulus' (28.7 %, 43.9 %) were also significantly enriched, with much more downregulated DEPs than upregulated DEPs involved. Further, TopGO analysis of enriched GO terms from BP (Figs. S2 and S3) also found that many immune-related GO terms were grouped in downregulated terms. Their topological relationships are shown in Fig. S2. In CC,

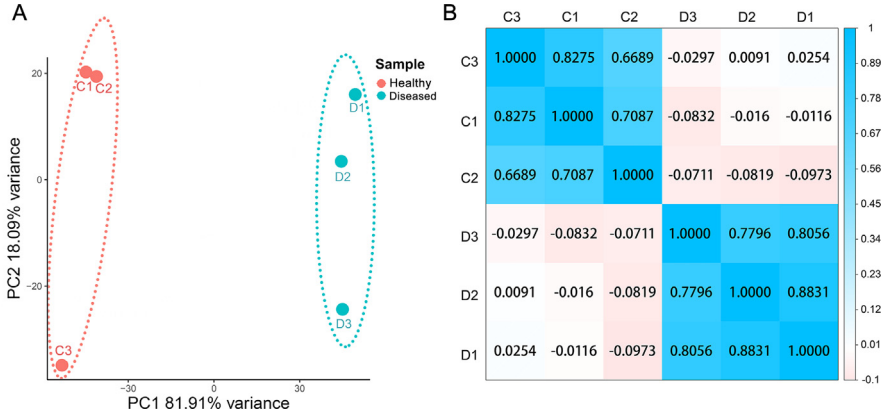

Fig. 2. Protein expression correlations among different samples from the diseased and healthy groups. A. Principal component analysis indicating clear differences between the diseased and healthy groups. B. Pearson correlation coefficients indicating good reproducibility of the duplicate samples from the two groups. Colours indicate the Pearson correlation coefficient values.

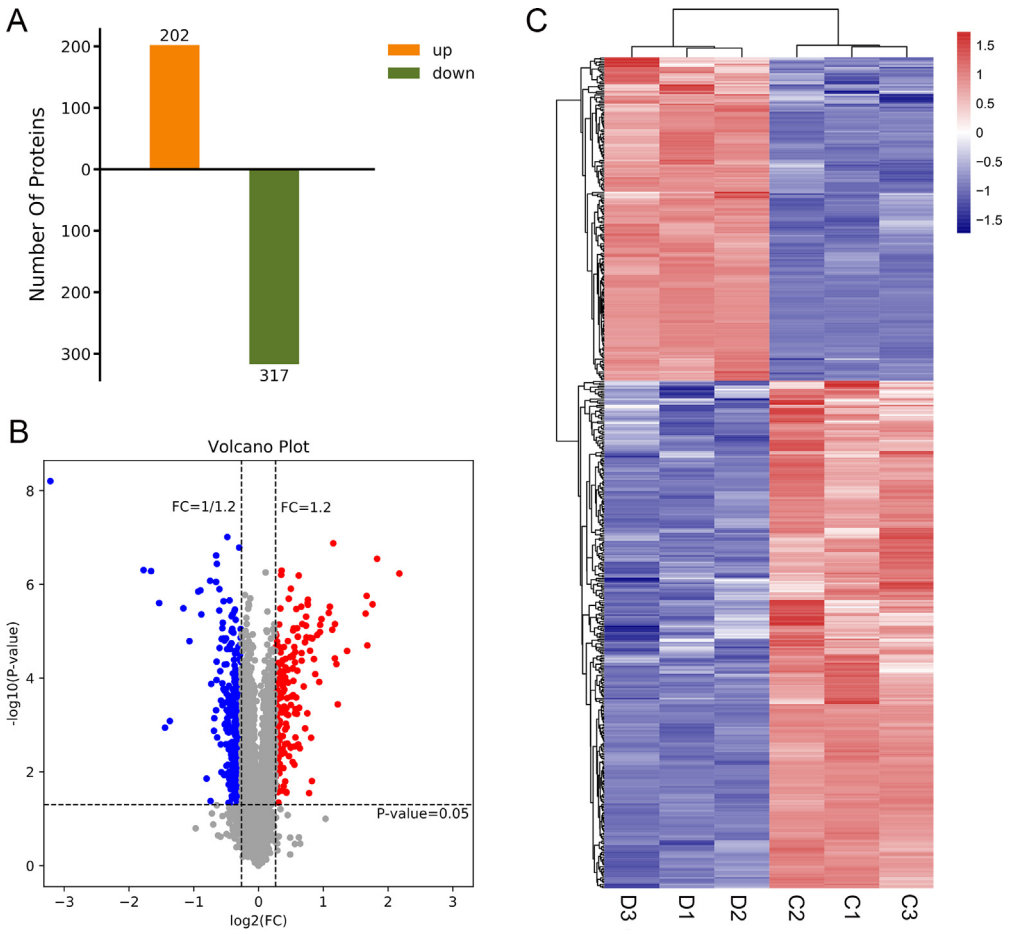

Fig. 3. Differentially expressed proteins (DEPs) modulated in the Yesso scallop in response to *Polydora* infection. A. Statistics of upregulated and downregulated DEPs ($p < 0.05$ and Foldchange $\geq$1.2 or $\leq$0.83) in the diseased group. B. Volcano plot showing the upregulated and downregulated DEPs (red and blue dots, respectively) in the diseased group. Grey dots indicate no significance change in expression level. C. Hierarchical clustering analysis showing a significant difference in protein expression between healthy and diseased Yesso scallops. The colour range indicates the protein expression levels, which are centralized between −1.5 and 1.5. Red and blue bars indicate upregulation and downregulation in the diseased group, respectively. (For interpretation of the references to colour in this figure legend, the reader is referred to the web version of this article.)

the most enriched functions were for 'cell' (79.0 %, 85.4 %), 'cell part' (79.0 %, 85.4 %) and 'organelle' (57.3 %, 66.9 %); besides, nervous system-related functions were also significantly enriched; i.e., 'synapse' (3.2 %,2.5 %) and 'synapse part' (1.9 %, 2.5 %; Fig. 4). Topology analysis for enriched GO terms from CC indicates that melanosome-, endoplasmic reticulum-, synapse- and membrane-related functions were significantly upregulated (Fig. S4), while lysosome-related functions were both up- and downregulated (Figs. S4 and S5). In MF, the most enriched functions were for 'binding' (56.1 %, 72.4 %), 'catalytic activity' (54.8 %, 49.4 %) and 'structural molecule activity' (5.7 %, 2.9 %). Topological graphs of the enriched terms involved in MF are shown in Figs. S6 and S7.

3.4. KEGG pathway analysis of DEPs

KEGG enrichment analysis was performed separately for the upregulated and downregulated DEPs using a threshold of protein number $\geq$2 and $p \leq 0.05$. For upregulated DEPs, a total of 25 pathways were detected as significantly enriched (Fig. 5A). Pathways involved in the process of phagocytosis, i.e., 'phagosome' (ko04145), 'lysosome' (ko04142) and 'antigen processing and presentation' (ko04612) were significantly enriched. The upregulated DEPs involved in these pathways are listed in Table 2. Besides, the melanin biosynthesis-related pathways of 'tyrosine metabolism (ko00350)' and 'melanogenesis (ko04916)' and the nervous system-related pathways of 'GABAergic synapse (ko04727)' and 'cholinergic synapse (ko04725)', were also significantly upregulated.

The downregulated DEPs also featured 25 pathways that were significantly enriched (Fig. 5B). 'Fc gamma R-mediated phagocytosis (ko04666)' was significantly enriched, which is due to the proteins involved in the processes of signal recognition and transduction (as listed in Table 2) being significantly downregulated. Many immune-related pathways, i.e., the 'RIG-I-like receptor signalling pathway (ko04622)', 'notch signalling pathway (ko04330)', 'TNF signalling pathway (ko04668)' and 'HIF-1 signalling pathway (ko04066)' showed significant downregulation. Further, the apoptotic pathways 'Apoptosis (ko04210)', 'Apoptosis-multiple species (ko04215)' and 'Apoptosis-fly (ko04214)' and the nervous system-related pathways 'serotonergic synapse' were also significantly enriched for downregulated DEPs.

3.5. Protein-protein interaction network analysis

A PPi network was constructed to obtain a global view of the interaction relationships of the DEPs, especially for those involved in response mechanisms. As shown in Fig. 6, DEPs associated with innate immunity, phagocytosis, melanization, apoptosis and the nervous system comprised a dense protein interaction network. Although the network still needs to be verified, it provides a nar-

Table 1
Candidate DEPs involved in the response to *Polydora* infection in the mantle tissue of Yesso scallops.

Accession No.	Description	Regulated	*p*	Foldchange
Melanization				
A0A210Q121	Cartilage matrix protein	Up	2.86E−07	3.56
A0A210QTH5	Temptin	Up	4.22E−06	3.15
A0A210QHS0	LaccasE−25	Up	3.91E−05	1.81
A0A210QI33	Cartilage matrix protein	Up	6.50E−07	1.54
A0A210Q5A2	Ferric-chelate reductase 1	Up	1.31E−05	1.52
A0A210Q6E6	Macrophage migration inhibitory factor	Up	8.63E−06	1.51
A0A210QKF2	Frizzled-1	Up	3.49E−05	1.44
A0A210QBL3	Collagen alpha-1(XIV) chain	Up	3.56E−05	1.40
A0A210PIX1	Collagen alpha-1(XII) chain	Up	2.03E−06	1.38
A0A210PR16	von Willebrand factor D and EGF domain-containing protein	Up	2.78E−02	1.35
A0A210R4S4	Chorion peroxidase	Up	3.95E−03	1.32
A0A210PE28	Calmodulin	Up	2.01E−02	1.31
A0A210Q5H7	Periostin	Up	2.52E−02	1.28
A0A210QSD2	Metalloproteinase inhibitor 2	Up	2.56E−04	1.28
A0A210QCG4	Calumenin-A	Up	5.50E−04	1.24
A0A210QLP2	Collagen alpha-5(VI) chain	Up	2.13E−05	1.24
A0A210QUX9	Carbonic anhydrase 2	Up	4.74E−05	1.24
A0A210PML5	Calmodulin	Up	2.69E−02	1.23
A0A210PZG9	Adenylate cyclase type 9	Up	1.09E−03	1.23
A0A210PS70	Metalloproteinase inhibitor 3	Up	6.60E−04	1.22
A0A210QV28	Aromatic-L-amino-acid decarboxylase	Up	1.38E−04	1.20
Innate immune response				
A0A210QGY2	Big defensin	Up	3.62E−04	2.34
A0A210R1T6	Glutathione S-transferase U26	Up	1.37E−05	1.74
A0A210PUG1	Glutathione S-transferase A	Up	1.35E−05	1.67
A0A210R780	Microsomal glutathione S-transferase 3	Up	5.81E−04	1.35
A0A210PZ65	Rhamnose-binding lectin	Up	1.08E−04	1.32
A0A1C9U318	Heat shock 70 kDa protein	Up	3.40E−03	1.28
A0A210R1B1	TNF_2 domain-containing protein	Up	9.25E−03	1.24
A0A210R6Y4	Myeloperoxidase	Up	1.32E−04	1.21
A0A210PZX6	Phosphotransferase	Down	2.00E−04	0.83
A0A210QZ89	Galectin	Down	1.92E−04	0.83
A0A210QAI4	Peroxiredoxin-2	Down	9.75E−04	0.83
A0A210R5V4	Interferon-induced helicase C domain-containing protein 1	Down	2.94E−04	0.83
A0A210PTS3	Interferon-induced protein 44	Down	2.94E−04	0.83
A0A210PIA4	Phosphotransferase	Down	6.90E−05	0.80
A0A210R1A3	TNF_2 domain-containing protein	Down	5.21E−03	0.79
A0A210R5I7	Thioredoxin	Down	7.00E−03	0.78
A0A210PPM0	Egl nine-like 1	Down	2.26E−02	0.77
A0A1C9U302	Heat shock 70 kDa protein	Down	4.28E−03	0.75
A0A1C9U2Y4	Heat shock 70 kDa protein	Down	4.00E−04	0.74
A0A210R7J8	PPE family protein PPE21	Down	3.46E−03	0.74
A0A210QEG4	Heat shock 70 kDa protein	Down	9.73E−04	0.70
A0A210Q2B5	ATP-dependent RNA helicase DDX58	Down	5.13E−05	0.70
A0A210PPR6	Glutathione S-transferase	Down	1.43E−06	0.52
Apoptosis				
A0A210PZ05	Caspase-2	Down	9.08E−03	0.83
A0A210QW88	Mitogen-activated protein kinase kinase kinase 15	Down	9.03E−03	0.82
A0A210PPU8	Caspase-9	Down	1.01E−04	0.81
A0A210Q8I6	Histone deacetylase 1	Down	1.86E−03	0.81
A0A210Q2I6	Inositol 1,4,5-trisphosphate receptor type 1	Down	8.20E−03	0.80
A0A210QD94	DNAation factor subunit beta	Down	1.54E−03	0.80
A0A210QR69	Dipeptidyl peptidase 1	Down	1.46E−02	0.79
A0A210QS38	Nicastrin	Down	2.37E−02	0.76
A0A210PPU3	Caspase-7	Down	3.29E−04	0.74
A0A210R4G5	Inhibitor of nuclear factor kappa-B kinase subunit epsilon	Down	1.16E−02	0.74
A0A210QPF7	Caspase-3	Down	1.72E−04	0.71
A0A210PWC2	Caspase-7	Down	4.75E−04	0.71
A0A210PJS9	Indoleamine 2,3-dioxygenase 1	Down	1.14E−03	0.37
Nervous system				
A0A210QLT3	Neurotrypsin	Up	1.17E−04	1.32
A0A210QBV2	Carboxylic ester hydrolase	Up	2.28E−04	1.23
A0A210PZG9	Adenylate cyclase type 9	Up	1.09E−03	1.23
A0A210Q4Q4	Low-density lipoprotein receptor-related protein 4	Up	4.31E−03	1.22
A0A210QZI0	Guanine nucleotide-binding protein subunit gamma	Up	2.24E−04	1.22
A0A210PYR6	E3 ubiquitin-protein ligase HERC2	Down	1.73E−02	0.83
A0A210QC59	Phospholipase A2	Down	3.47E−04	0.83
A0A210Q2I6	Inositol 1,4,5-trisphosphate receptor type 1	Down	8.20E−03	0.80
A0A210QL83	Syntaxin-18	Down	1.11E−04	0.80
A0A210Q6A1	Arachidonate 5-lipoxygenase	Down	2.98E−05	0.78
A0A210PHF5	Arachidonate 5-lipoxygenase	Down	1.51E−03	0.78
A0A210Q643	Allene oxide synthase-lipoxygenase protein	Down	9.79E−08	0.72

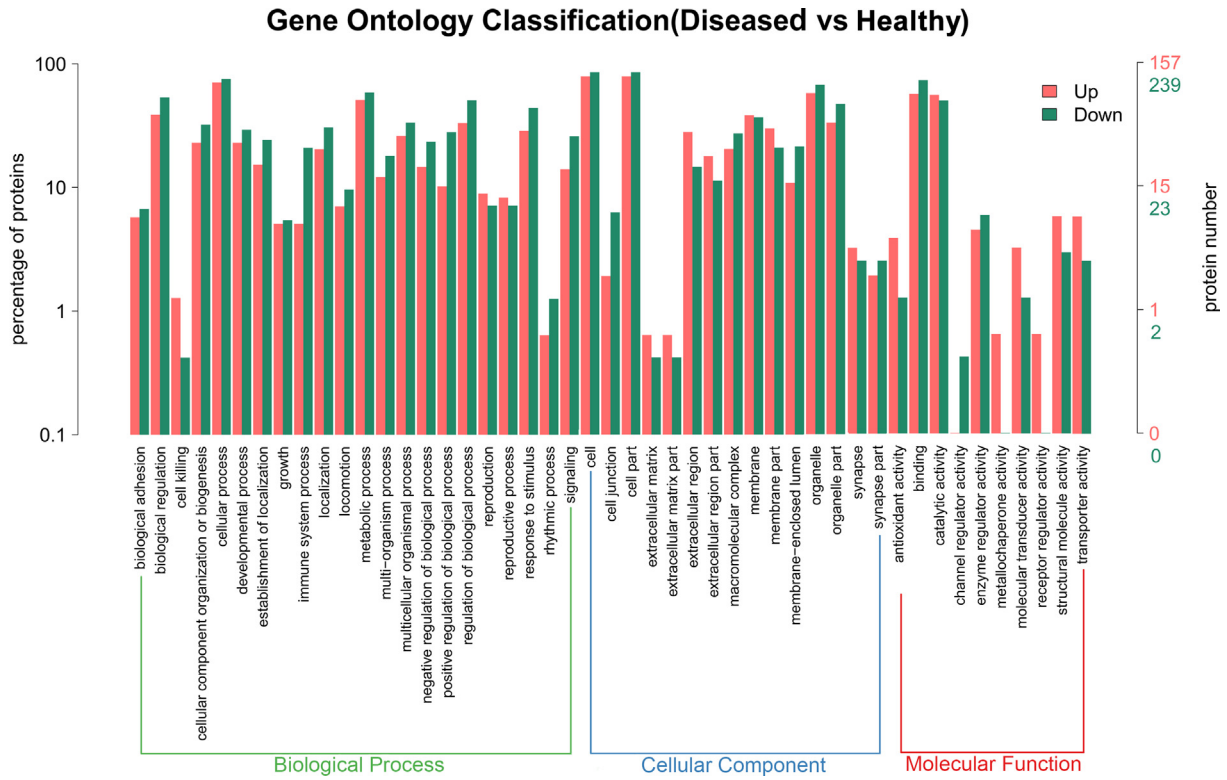

Fig. 4. Distribution of significantly enriched GO functions (level 2) for upregulated and downregulated DEPs in *Polydora*-infected Yesso scallops. The *x*-axis represents the biological functions of biological process, cellular component, and molecular function. The *y*-axis represents the percentage or number of proteins categorized into different functions.

row pool of protein–protein interactions, which probably contributes to the cooperation and coordination of their functions responding to *Polydora* infection.

3.6. Expression levels of genes involved in phagocytosis

The mRNA expression levels of genes encoding DEPs involved in phagocytosis, as listed in Table 2, were further detected by qRT-PCR. As shown in Fig. 7, the level of mRNA expression varied in parallel to the corresponding protein expression for all these genes. The expression levels of genes *TLR6*, *Integrin β3*, *Calnexin*, *V-ATPase*, *Cathepsin B*, *Cathepsin L*, *LPP*, *M6PR* and *GM2A*, which are involved in different stages of phagocytosis, were significantly upregulated in diseased Yesso scallops. The expression levels of genes involved in the FcγR-mediated signalling pathway, i.e., *SHIP2*, *BIN1*, *PKC* and *PAK1*, were significantly downregulated in diseased scallops.

4. Discussion

Polydora infection is one of the most serious diseases in the Yesso scallop and is also very common in other molluscan species [3–5]. However, few studies have focused on this disease, and the molecular response mechanisms of scallops are largely unknown. Proteins are the executors of various life functions, so a study of protein profiling changes in diseased Yesso scallops is necessary to elucidate their underlying molecular response mechanisms. Recently developed quantitative proteomic technology has provided effective and reliable methods for this. In the present study, a systematic proteome analysis was performed for the mantle tissues of *Polydora*-infected and healthy Yesso scallops using TMT-based technology. The key proteins and molecular pathways involved in the response mechanism were obtained, which predicted the molecular mechanism of the *Polydora*-infection response in Yesso scallops.

Scallops rely on an exclusively innate immune system to execute cellular and humoral immune reactions to invaders [9]. After *Polydora* infection, 519 proteins were detected as being differentially expressed in the mantle tissue of the Yesso scallop. Many immune-related GO functions and KEGG pathways were significantly enriched, indicating that immunomodulation is involved in the response mechanism of Yesso scallops. However, many of these functions and pathways were downregulated excepting those associated with phagocytosis, such as the pathways of ‘phagosome’ (ko04145), ‘lysosome’ (ko04142) and ‘antigen processing and presentation’ (ko04612). This suggests that phagocytosis probably played a major role in the immune response of Yesso scallops to *Polydora* infection. Phagocytosis is an indispensable cellular mechanism for recognizing and ingesting foreign molecules and cell debris, which are important in the innate and adaptive immunity of animals [26–29]. The process of phagocytosis is extremely complex and includes phagocytic receptor recognition, signalling pathway activation, focal cytoskeletal rearrangement, membrane fusion/fission, phagosome formation and maturation, and pathogen killing and degradation, which have been well studied in mammals [29–31]. Though studies have revealed that phagocytosis is one of the most pivotal cellular defence mechanisms in the innate immunity of scallops, its molecular composition and specific process are far from being well understood [9]. In the present study, DEPs involved in different stages of phagocytosis were identified from significantly enriched pathways (Fig. 7) which, for the first time, provides a global view of the molecular compositions of phagocytosis and their potential functions in scallops.

Phagocytosis starts with the binding of pathogens by specific receptors in the cell membrane. Dozens of receptors, such as FcγRs,

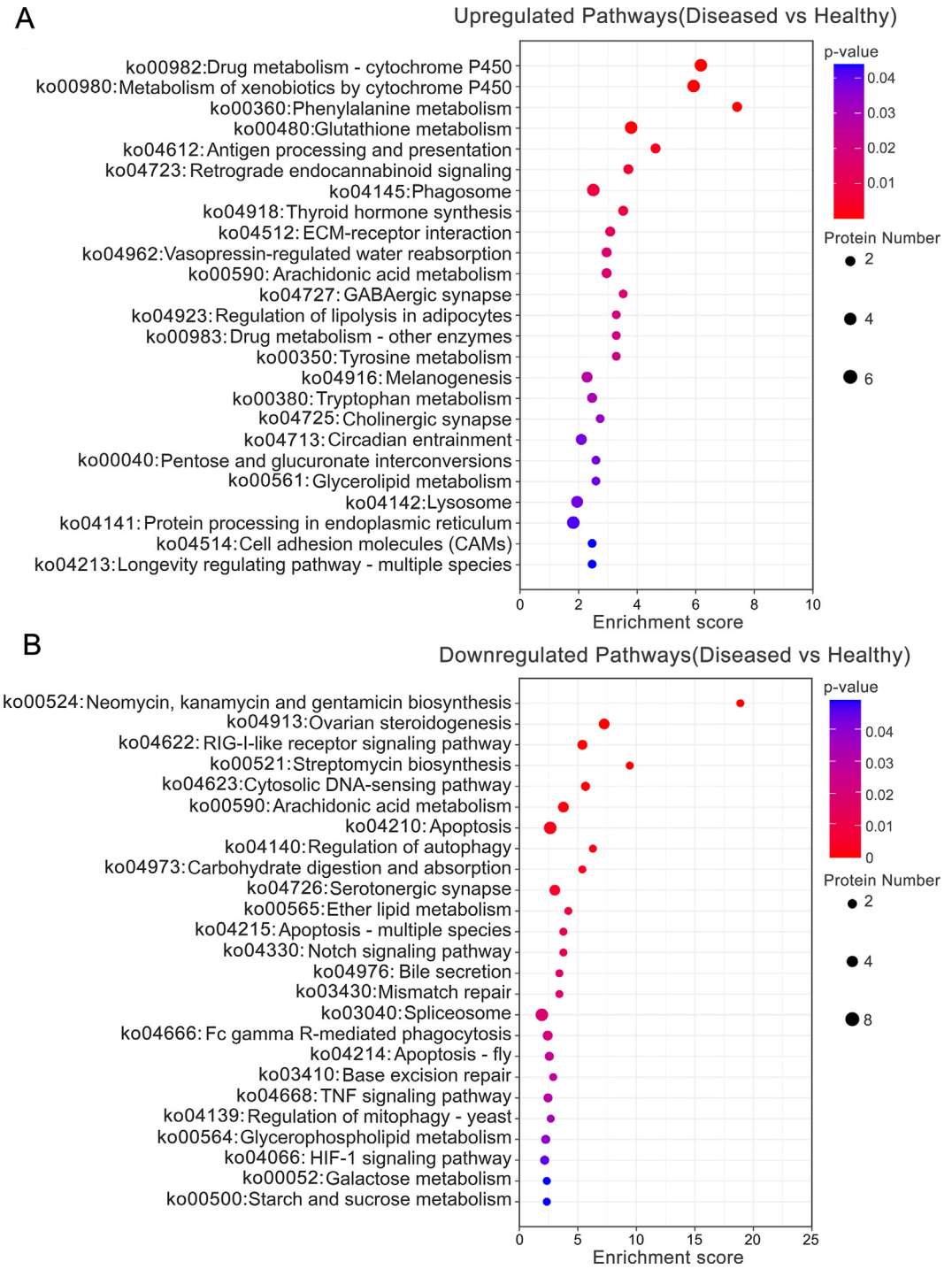

Fig. 5. KEGG enrichment analysis showing the significantly enriched pathways for upregulated (A) and downregulated (B) DEPs in *Polydora*-infected Yesso scallops. The *x*-axis shows the enrichment score. The left *y*-axis shows the KEGG pathway. The colour and size of each point represent the *p*-values and numbers of proteins enriched in a particular pathway.

CRs, lectins, TLRs, Integrins and so on, have been implicated in phagocytosis as sensing and responding to different pathogens in vertebrates [31–35]. Among these receptors, FcγRs are a classic receptor that mediates signal transduction events to internalize immunoglobulin-bound particles [33,36–37]. However, the FcγR-mediated signalling pathway was significantly downregulated in diseased Yesso scallops in the present study. In contrast, another two types of receptors of TLR6 and Integrin β3 identified in the 'phagosome (ko04145)' pathway were significantly upregulated. Although controversy has existed regarding the function of TLRs in phagosome maturation, many studies have indicated that TLRs can positively regulate phagocytosis [35,38–42]. They are probably engaged as sensor receptors and often collaborate with other receptors to promote uptake and downstream signalling [29,32,43–45]. Integrins are expressed at the surface of most metazoan cells, and integrin-dependent phagocytosis is emerging as a general and intrinsic ability of most integrins [34,46–48]. Studies in mammals have also determined that integrins can cooperate with TLRs to enhance phagocytosis [44]. Therefore, the simultaneously upregulation of TLR6 and Integrin β3 in both mRNA and pro-

Table 2
Information on the DEPs involved in the phagocytosis pathway.

Accession No.	Description	Regulated	Gene		Protein		Pathway
			p	Foldchange	*p*	Foldchange	
A0A210Q910	Toll-like receptor 6 (TLR6)	Up	1.67E−02	2.46	4.45E−04	1.21	ko04145
A0A210Q793	Integrin beta pat-3 (Integrin β3)	Up	6.66E−03	2.33	6.22E−04	1.22	ko04145
A0A210PH61	V-type proton ATPase subunit G 1 (V-ATPase)	Up	2.29E−01	1.31	1.24E−04	1.37	ko04145
A0A210QC09	Calnexin	Up	4.16E−02	2.85	4.82E−04	1.25	ko04145; ko04612
A0A210PQX0	Cathepsin B	Up	1.67E−02	2.42	5.66E−04	1.23	ko04142; ko04612
A0A210QXK9	Cathepsin L	Up	7.93E−03	2.34	2.50E-03	1.36	ko04145; ko04142; ko04612
A0A210PG74	Cation-dependent mannose-6-phosphate receptor (M6PR)	Up	1.58E−02	3.07	9.33E−04	1.34	ko04145; ko04142
A0A210Q6B2	Ganglioside GM2 activator (GM2A)	Up	4.94E−02	5.11	1.77E−06	3.18	ko04142
A0A210QH63	Lysosomal protective protein (LPP)	Up	4.42E−02	2.14	2.61E−03	1.23	ko04142
A0A210PWQ3	Phosphatidylinositol 3,4,5-trisphosphate 5-phosphatase 2 (SHIP2)	Down	4.11E−02	0.69	3.59E−02	0.82	ko04666
A0A210PC53	Myc box-dependent-interacting protein 1 (BIN1)	Down	2.04E−02	0.51	1.72E−04	0.70	ko04666
A0A210PF28	Protein kinase C delta type (PKC)	Down	1.44E−02	0.33	6.03E−04	0.82	ko04666
A0A210Q2L3	Serine/threonine-protein kinase PAK 1 (PAK1)	Down	2.98E−02	0.50	1.15E−04	0.83	ko04666

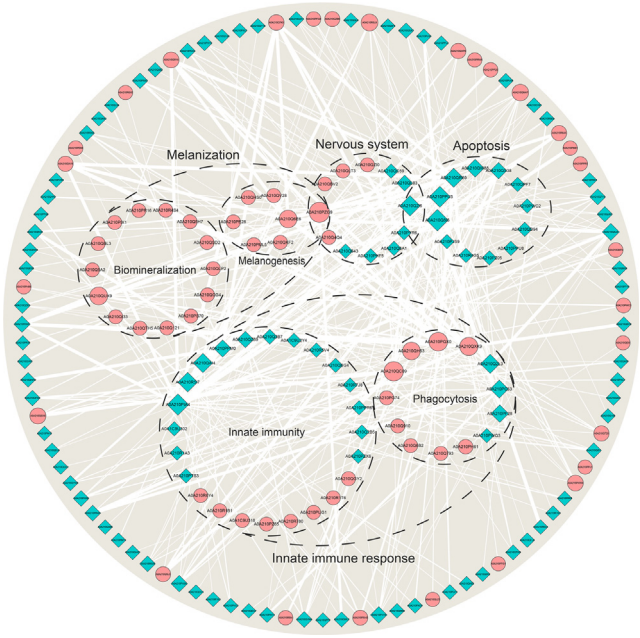

Fig. 6. Protein-protein interaction (PPi) network of DEPs in diseased and healthy Yesso scallops. Red circles represent upregulated DEPs, the blue squares represent downregulated DEPs, and the size of the two graphs indicates the number of interacting proteins. The width of the lines indicates the protein interaction evaluation score. (For interpretation of the references to colour in this figure legend, the reader is referred to the web version of this article.)

tein levels in diseased Yesso scallops suggested that TLR6 or/and Integrin, rather than FcγRs, probably serve as the main receptors recognizing *Polydora* infection. They might cooperate with each other to enhance phagocytosis, considering the complex phagocytic targets that occur during *Polydora* infection. However, the mechanism of cooperation between these two receptors requires further investigation in scallops.

ER-mediated phagocytosis, despite being a recently proposed model, seems to be a general mechanism of phagocytosis [30,31], but has never been reported in molluscs. ER has been proven to be an important source of membrane involved in phagosome biogenesis, which is required to overcome the consumption of cell surface membrane during phagocytosis [30,31,49]. One of the strongest pieces of evidence for this model is the discovery of several ER-resident proteins (such as Calnexin) in phagosomes [30,31,50–51]. In the present study, GO functions in CC related to membrane and ER were significantly enriched and upregulated in diseased scallops, which indicates an important role of ER in disease response. Further, significantly higher mRNA and protein expression levels of the ER-specific protein, Calnexin, were detected in diseased scallops. The Ca^{2+} storage capacity of Calnexin might directly modulate the activities of the actin system and affect the uptake of pathogens into phagosomes [50]. Though direct evidence is still needed, the present results, to some extent, indicate that ER-mediated phagocytosis probably occurrs in Yesso scallops in response to *Polydora* infection, which is the first such viewpoint proposed in molluscs.

After invagination of the plasma membrane to trap pathogens in a newly formed phagosome, the vesicle engages in a maturation process where it fuses with various organelles, such as lysosomes. It finally forms a matured phagolysosome that is able to kill and degrade pathogens by using proteolytic enzymes in an extremely acidic environment [29–31]. V-ATPase, acting as a molecular pump that generates proton gradients, is responsible for making the pH of phagosomes fall as low as 4.0–4.5 [29,52–53]. In the present study, both the mRNA and protein of V-ATPase showed higher expression levels in *Polydora*-infected scallops than in healthy ones, although significant differences were only detected in protein expressions. The results indicate that acidification of phagosomes mediated by V-ATPase might also occur in the phagocytosis of scallops, which is essential for killing pathogens. Besides, the GO functions and KEGG pathways related to lysosomes were significantly enriched, and many lysosomal proteins, such as Cathepsin B, Cathepsin L, LPP, M6PR and GM2A, were significantly upregulated in both mRNA and protein levels in diseased Yesso scallops. This hints that there is involvement of lysosomes in phagocytosis in scallops. The fusion with lysosomes will provide essential enzymes for phagosomes to ingest and degrade pathogens [31,49]. Cathepsins are a group of important proteolytic enzymes containing many different members, such as Cathepsin A, B, D, L, S and Z, which have been detected in phagosomes [31,49,54–57]. In this study, Cathepsin B and L probably played important roles in pathogen killing as there were significantly upregulated mRNA and protein expression levels of these two genes in diseased Yesso scallops.

Besides phagocytosis, the melanization response of the mantle probably also plays a vital function in *Polydora*-infected Yesso scallops. Firstly, melanizaition of the shell is an obvious trait of *Polydora*-infected individuals (Fig. 1). Further, melanization-related GO functions of 'melanosome (GO:0042470)' and the KEGG pathways of 'tyrosine metabolism (ko00350)' and 'melanogenesis (ko04916)' were significantly enriched for upregulated DEPs,

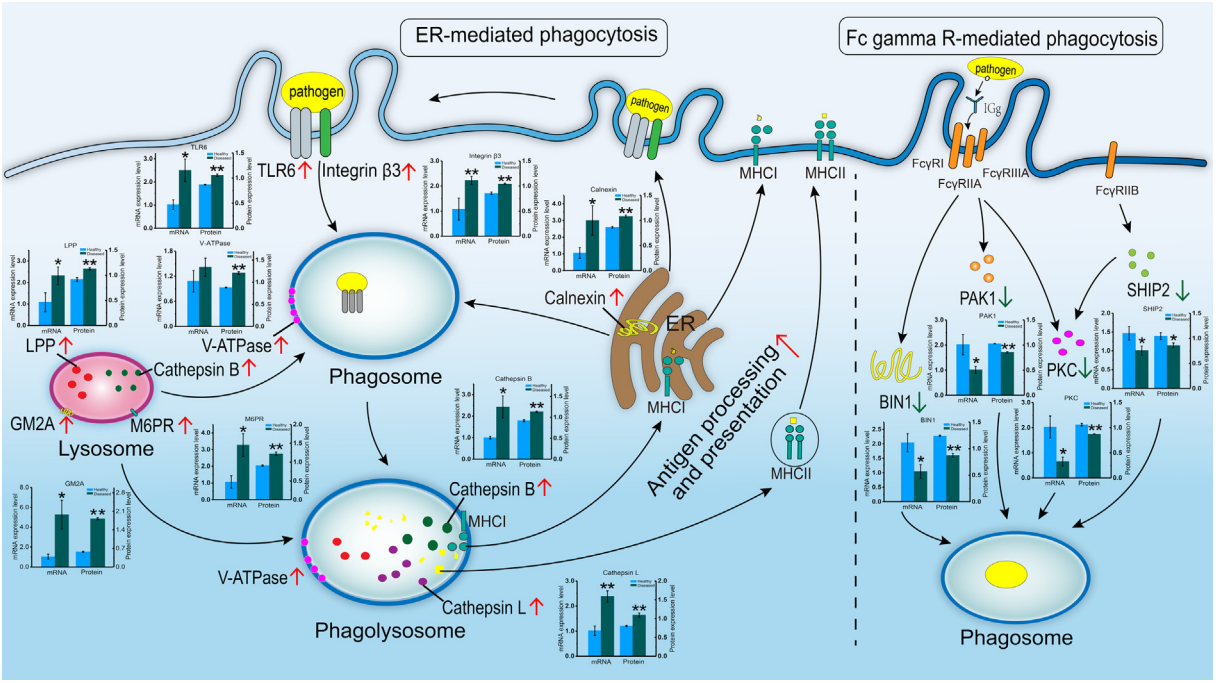

Fig. 7. Phagocytosis pathway in the Yesso scallop in response to *Polydora* infection. The mRNA and protein expression levels of DEPs involved in phagocytosis are presented as means ± standard error (n = 3). Asterisks indicate significant differences ($^{*}p < 0.05$, $^{**}p < 0.01$). Red and green arrows indicate upregulation and downregulation in *Polydora*-infected scallops, respectively. (For interpretation of the references to colour in this figure legend, the reader is referred to the web version of this article.)

which supports this assumption molecularly. Melanization is a normal process during shell formation in molluscs, but it is also an important mechanism involved in wound healing and encapsulation of foreign entities in invertebrates [13], and mantle epithelia have been shown to be mainly responsible for melanization [13]. The *Roseovarius* oyster disease (ROD) and brown ring disease (BRD) in clams are two other cases where mantle tissues produce copious amounts of melanins to wall off pathogens [58–59]. Melanin biosynthesis is highly regulated by a diverse group of enzymes generally named phenoloxidases [13,60]. Laccase is one of these enzymes, which has been shown to be upregulated in the mantle of clams affected by BRD [61]. Similar results were also found in the present study: a significant increase in the protein expression level of a laccase was detected in *Polydora*-infected scallops. Sometimes, melanization is accompanied by a biomineralization mechanism to embed melanized invaders in new calcified shell layers, leading to major rearrangements of the shell matrix, as found in ROD and BRD [13,58,59,61]. In the present study, some biomineralization directly associated proteins, such as Cartilage matrix protein, Temptin, Periostin, Collagen, Calmodulin, Calumenin-A and so on, were markedly upregulated. This probably indicates that there is accelerated secretion of shell matrix in mantle tissues to resist *Polydora* infection or repair damaged shell structures.

In addition, inhibition of apoptosis and neural modulation may be also involved in the response mechanism. Apoptosis is a vital mechanism in regulating cell numbers throughout the life of all metazoan animals. The most fundamental biochemical event in apoptosis is the participation of caspases, which exist in two main groups: initiators and executioners [62–64]. In the present study, the apoptosis pathways were enriched among the downregulated DEPs, which were mainly caused by the significantly downregulated caspases, including caspase 2, caspase 9 as activators, and caspase 3 and caspase 7 as executioners [64]. Molecularly, the results suggest inhibition of the apoptosis process in the mantle tissues of infected Yesso scallops, which is probably closely associated with the obviously increased mucous cells in the mantle, as observed in our previous study [14]. Finally, the nervous system may participate in the modulation of Yesso scallops' response to *Polydora* infection. There were significantly enriched synaptic GO functions and KEGG pathways among the DEPs, and the protein expression levels of some nervous system-related proteins were differentially regulated. Extraordinarily developed nervous fibres are distributed in the mantle of scallops, making the tissue sensitive to external intrusion and able to regulate a rapid response [14].

5. Conclusion

In the present study, a systematic proteome analysis of the mantle tissues of *Polydora*-infected and healthy Yesso scallops was performed by TMT technology. DEPs were detected and further analysed by GO and KEGG enrichment analysis. The results indicate that the phagocytosis pathway was significantly upregulated in the diseased group. DEPs involved in different stages of phagocytosis were discovered and further verified by qRT-PCR, suggesting an important role of this pathway in response to *Polydora* infection. Besides, proteins involved in melanization, apoptosis and nervous modulation were also found to be significantly regulated and enriched, indicating their involvement in the infection response. Finally, a PPi network was constructed to provide a global view of the interaction relationships of the DEPs. This study provides insights into the molecular mechanism of the Yesso scallop in response to *Polydora* infection, which will help to better comprehend the innate immune mechanisms of molluscs and lay a significant theoretical foundation for *Polydora* disease control.

CRediT authorship contribution statement

Hongyan Sun: Resources, Investigation, Formal analysis, Visualization, Validation, Writing – original draft. **Junxia Mao:** Conceptualization, Formal analysis, Visualization, Data curation, Writing –

original draft, Funding acquisition. **Yiying Wang:** Resources, Investigation, Validation. **Zhiyue Fan:** Investigation, Validation. **Changzi Yuan:** Investigation. **Xubo Wang:** Resources. **Ying Tian:** Formal analysis. **Bing Han:** Formal analysis. **Zhenlin Hao:** Writing – review & editing. **Jun Ding:** Writing – review & editing. **Yaqing Chang:** Supervision, Writing – review & editing, Funding acquisition.

Declaration of Competing Interest

The authors declare that they have no known competing financial interests or personal relationships that could have appeared to influence the work reported in this paper.

Acknowledgements

This project was supported by the Science and Technology Foundation of Dalian (2021JB11SN035), the Scientific Research Fund of the Liaoning Provincial Department of Education (LJKZ0705), the Dalian High-level Talent Innovation Support Program (2019RQ143), and the National Natural Science Foundation of China (31702342).

Appendix A. Supplementary data

Supplementary data to this article can be found online at https://doi.org/10.1016/j.csbj.2022.10.043.

References

[1] Kosaka Y, Ito H. *Patinopecten (Mizuhopecten) yessoensis*. In: Shumway S, Parsons GJG, editors. Scallops: biology, ecology and aquaculture and fisheries. Amsterdam: Elsevier; 2016. p. 891–925.
[2] Wang Q. Introduction of Japanese scallop and prospect of culture it in northern China. Fish Sci 1984;3(4):24–7. https://doi.org/10.16378/j.cnki.1003-1111.1984.04.008.
[3] Sato-Okoshi W, Nomura T. Infestation of the Japanese scallop *Patinopecten yessoensis* by the boring polychaetes *Polydora* on the coast of Hokkaido and Tohoku district. Nippon Suisan Gakkaishi 1985;51(3):371–80. https://doi.org/10.2331/suisan.51.371.
[4] Mortensen S, Meeren T, Fosshagen A, Hernar I, Harkestad L, Torkildsen L, et al. Mortality of scallop spat in cultivation, infested with tube dwelling bristle worms Polydora sp.. Aquacult Int 2000;8(2):267–71. https://doi.org/10.1023/a:1009287706756.
[5] Getchell RG, Smolowitz RM, McGladdery SE, Bower SM. Diseases and parasites of scallops. In: Shumway S, Parsons GJG, editors. Scallops: biology, ecology, aquaculture, and fisheries. Amsterdam: Elsevier; 2016. p. 425–52.
[6] Sato-Okoshi W, Okoshi K. Microstructure of scallop and oyster shells infested with boring *Polydora*. Nippon Suisan Gakkaishi 1993;59(7):1243–7. https://doi.org/10.2331/suisan.59.1243.
[7] Sato-Okoshi W, Okoshi K. Structural characteristics of self-excavated burrows by boring polydorid species (Polychaeta, Spionidae). Bull Mar Sci 2000;67(1):235–48.
[8] Silina AV. Tumor-like formations on the shells of Japanese scallops *Patinopecten yessoensis* (Jay). Mar Biol 2006;148(4):833–40. https://doi.org/10.1007/s00227-005-0120-4.
[9] Song L, Wang L, Zhang H, Wang M. The immune system and its modulation mechanism in scallop. Fish Shellfish Immunol 2015;46(1):65–78. https://doi.org/10.1016/j.fsi.2015.03.013.
[10] Audino JA, Marian JEAR, Wanninger A, Lopes SBC. Mantle margin morphogenesis in *Nodipecten nodosus* (Mollusca: Bivalvia): new insights into the development and the roles of bivalve pallial folds. BMC Dev Biol 2015;15(1):1–22. https://doi.org/10.1186/s12861-015-0074-9.
[11] Checa A. A new model for periostracum and shell formation in *Unionidae* (Bivalvia, Mollusca). Tissue Cell 2000;32(5):405–16. https://doi.org/10.1054/tice.2000.0129.
[12] Huang J, Li L, Jiang T, Xie L, Zhang R. Mantle tissue in the pearl oyster *Pinctada fucata secretes* immune components via vesicle transportation. Fish Shellfish Immunol 2022;121:116–23. https://doi.org/10.1016/j.fsi.2022.01.001.
[13] Allam B, Espinosa EP. Mucosal immunity in mollusks. In: Beck BH, Peatman E, editors. Mucosal health in aquaculture. Salt Lake City, UT, USA: Academic Press; 2015. p. 325–50.
[14] Zhang W, Mao J, Yuan C, Yang J, Han B, Wang X, et al. Histological changes in the mantle tissue of the Yesso Scallop *Patinopecten yessoensis* shell infested by *Polydora*. J Shellfish Res 2020;39(1):87–97. https://doi.org/10.2983/035.039.0109.
[15] Aslam B, Basit M, Nisar MA, Khurshid M, Rasool MH. Proteomics: technologies and their applications. J Chromatogr Sci 2017;55(2):182–96. https://doi.org/10.1093/chromsci/bmw167.
[16] Yu Z, Hong X, Zhang X, Zheng F, Liu F, Xu H, et al. Global proteomic analyses reveals abnormal immune regulation in patients with new onset Ankylosing Spondylitis. Front Immunol 2022;13:. https://doi.org/10.3389/fimmu.2022.838891838891.
[17] Saco A, Panebianco A, Blanco S, Novoa B, Diz AP, Figueras A. Integration of transcriptomics and proteomics improves the characterization of the role of mussel gills in a bacterial waterborne infection. Front Mar Sci 2021;8:. https://doi.org/10.3389/fmars.2021.735309735309.
[18] Sun J, Zhang Y, Thiyagarajan V, Qian P, Qiu J. Protein expression during the embryonic development of a gastropod. Proteomics 2010;10(14):2701–11. https://doi.org/10.1002/pmic.200900846.
[19] Martínez-Fernández M, Rodríguez-Piñeiro AM, Oliveira E, Páez de la Cadena M, Rolán-Alvarez E. Proteomic comparison between two marine snail ecotypes reveals details about the biochemistry of adaptation. J Proteome Res 2008;7(11):4926–34. https://doi.org/10.1021/pr700863e.
[20] Di G, Luo X, You W, Zhao J, Kong X, Ke C. Proteomic analysis of muscle between hybrid abalone and parental lines *Haliotis gigantea* Reeve and *Haliotis discus hannai* Ino. Heredity 2015;114(6):564–74. https://doi.org/10.1038/hdy.2014.124.
[21] Thompson A, Schäfer J, Kuhn K, Kienle S, Schwarz J, Schmidt G, et al. Tandem mass tags: a novel quantification strategy for comparative analysis of complex protein mixtures by MS/MS. Anal Chem 2003;75(8):1895–904. https://doi.org/10.1021/ac0262560.
[22] Wang S, Zhang J, Jiao W, Xun X, Guo X, Dong B, et al. Scallop genome provides insights into evolution of bilaterian karyotype and development. Nat Ecol Evol 2017;1(5):1–12. https://doi.org/10.1038/s41559-017-0120.
[23] Yuan C, Mao J, Sun H, Wang X, Tian Y, Song J, et al. Genome-wide identification and characterization of Pif genes in the Yesso scallop (*Patinopecten yessoensis*), and their expression patterns in response to *Polydora* shell infestation. Aquaculture 2021;545:. https://doi.org/10.1016/j.aquaculture.2021.737223737223.
[24] Feng L, Yu Q, Li X, Ning X, Wang J, Zou J, et al. Identification of reference genes for qRT-PCR analysis in Yesso Scallop *Patinopecten yessoensis*. PLoS ONE 2013;8(9):e75609.
[25] Livak KJ, Schmittgen TD. Analysis of relative gene expression data using Real-Time quantitative PCR. Methods 2001;25(4):402–8. https://doi.org/10.1006/meth.2001.
[26] Brown EJ. Phagocytosis. BioEssays 1995;17(2):109–17. https://doi.org/10.1002/bies.950170206.
[27] Jutras I, Desjardins M. Phagocytosis: at the crossroads of innate and adaptive immunity. Annu Rev Cell Dev Biol 2005;21(1):511–27. https://doi.org/10.1146/annurev.cellbio.20.010403.102755.
[28] Rosales C, Uribe-Querol E. Phagocytosis: a fundamental process in immunity. Biomed Res Int 2017;2017:1–18. https://doi.org/10.1155/2017/9042851.
[29] Gordon S. Phagocytosis: an immunobiologic process. Immunity 2016;44(3):463–75. https://doi.org/10.1016/j.immuni.2016.02.026.
[30] Gagnon E, Duclos S, Rondeau C, Chevet E, Cameron PH, Steele-Mortimer O, et al. Endoplasmic reticulum-mediated phagocytosis is a mechanism of entry into macrophages. Cell 2002;110(1):119–31. https://doi.org/10.1016/S0092-8674(02)00797-3.
[31] Desjardins M. ER-mediated phagocytosis: a new membrane for new functions. Nat Rev Immunol 2003;3(4):280–91. https://doi.org/10.1038/nri1053.
[32] Dill BD, Gierlinski M, Härtlova A, Arandilla AG, Guo M, Clarke RG, et al. Quantitative proteome analysis of temporally resolved phagosomes following uptake via key phagocytic receptors[S]. Mol Cell Proteomics 2015;14(5):1334–49. https://doi.org/10.1074/mcp.M114.044594.
[33] Goodridge HS, Underhill DM, Touret N. Mechanisms of Fc receptor and dectin-1 activation for phagocytosis. Traffic 2012;13(8):1062–71. https://doi.org/10.1111/j.1600-0854.2012.01382.x.
[34] Freeman SA, Goyette J, Furuya W, Woods EC, Bertozzi CR, Bergmeier W, et al. Integrins form an expanding diffusional barrier that coordinates phagocytosis. Cell 2016;164(1–2):128–40. https://doi.org/10.1016/j.cell.2015.11.048.
[35] Blander JM, Medzhitov R. Regulation of phagosome maturation by signals from toll-like receptors. Science 2004;304(5673):1014–8. https://doi.org/10.1126/science.1096158.
[36] Swanson JA, Hoppe AD. The coordination of signaling during Fc receptor-mediated phagocytosis. J Leukoc Biol 2004;76(6):1093–103. https://doi.org/10.1189/jlb.0804439.
[37] Van Zon JS, Tzircotis G, Caron E, Howard M. A mechanical bottleneck explains the variation in cup growth during FcγR phagocytosis. Mol Syst Biol 2009;5(1):298. https://doi.org/10.1038/msb.2009.59.
[38] Russell DG, Yates RM. Toll-like receptors and phagosome maturation. Nat Immunol 2007;8(3):217. https://doi.org/10.1038/ni0307-217a.
[39] Blander JM, Medzhitov R. On regulation of phagosome maturation and antigen presentation. Nat Immunol 2006;7(10):1029–35. https://doi.org/10.1038/ni1006-1029.
[40] Underhill DM, Ozinsky A, Hajjar AM, Stevens A, Wilson CB, Bassetti M, et al. The toll-like receptor 2 is recruited to macrophage phagosomes and discriminates between pathogens. Nature 1999;401(6755):811–5. https://doi.org/10.1038/44605.
[41] Roy R, Singh SK, Das M, Tripathi A, Dwivedi PD. Toll-like receptor 6 mediated inflammatory and functional responses of zinc oxide nanoparticles primed macrophages. Immunology 2014;142(3):453–64. https://doi.org/10.1111/imm.12276.

[42] Underhill DM. Macrophage recognition of zymosan particles. J *Endotoxin Res* 2003;9(3):176–80. https://doi.org/10.1177/09680519030090030601.
[43] Henneke P, Takeuchi O, van Strijp JA, Guttormsen HK, Smith JA, Schromm AB, et al. Novel engagement of CD14 and multiple toll-like receptors by group B streptococci. J Immunol 2001;167(12):7069–76. https://doi.org/10.4049/jimmunol.167.12.7069.
[44] Fei D, Meng X, Yu W, Yang S, Song N, Cao Y, et al. Fibronectin (FN) cooperated with TLR2/TLR4 receptor to promote innate immune responses of macrophages via binding to integrin β1. Virulence 2018;9(1):1588–600. https://doi.org/10.1080/21505594.2018.1528841.
[45] Li W, Li M, Anthony SM, Yan Y. Spatial organization of FcγR and TLR2/1 on phagosome membranes differentially regulates their synergistic and inhibitory receptor crosstalk. Sci Rep 2021;11(1):1–11. https://doi.org/10.1038/s41598-021-92910-9.
[46] Nolte MA, Nolte ENM, Margadant C. Integrins control vesicular trafficking; new tricks for old dogs. Trends Biochem Sci 2021;46(2):124–37. https://doi.org/10.1016/j.tibs.2020.09.001.
[47] Dupuy AG, Caron E. Integrin-dependent phagocytosis–spreading from microadhesion to new concepts. J Cell Sci 2008;121(11):1773–83. https://doi.org/10.1242/jcs.018036.
[48] Torres-Gomez A, Cabañas C, Lafuente EM. Phagocytic integrins: activation and signaling. Front Immunol 2020;11:738. https://doi.org/10.3389/fimmu.2020.00738.
[49] Garin J, Diez R, Kieffer S, Dermine JF, Duclos S, Gagnon E, et al. The phagosome proteome: insight into phagosome functions. J Cell Biol 2001;152(1):165–80. https://doi.org/10.1083/jcb.152.1.165.
[50] Müller-Taubenberger A, Lupas AN, Li H, Ecke M, Simmeth E, Gerisch G. Calreticulin and calnexin in the endoplasmic reticulum are important for phagocytosi. EMBO J 2001;20(23):6772–82. https://doi.org/10.1093/emboj/20.23.6772.
[51] Campbell-Valois F X, Trost M, Chemali M, Dill B D, Laplante A, Duclos S, et al. Quantitative proteomics reveals that only a subset of the endoplasmic reticulum contributes to the phagosome. *Mol Cell Proteomics* (2012) 11(7): M111. 016378-1-M111. 016378-13. doi: 10.1074/mcp.m111.016378.
[52] Kissing S, Hermsen C, Repnik U, Nesset CK, Von Bargen K, Griffiths G, et al. Vacuolar ATPase in phagosome-lysosome fusion. J Biol Chem 2015;290 (22):14166–80. https://doi.org/10.1074/jbc.M114.628891.
[53] Hooper K M, Jacquin E, Li T, Goodwin J M, Brumell J H, Durgan, J, et al. V-ATPase is a universal regulator of LC3 associated phagocytosis and non-canonical autophagy. *bioRxiv* (2021) doi: 10.1101/2021.05.20.444917.
[54] Banati RB, Rothe G, Valet G, Kreutzberg GW. Detection of lysosomal cysteine proteinases in microglia: flow cytometric measurement and histochemical localization of cathepsin B and L. Glia 1993;7(2):183–91. https://doi.org/10.1002/glia.440070208.
[55] Porter K, Lin Y, Liton PB. Cathepsin B is up-regulated and mediates extracellular matrix degradation in trabecular meshwork cells following phagocytic challenge. PLoS ONE 2013;8(7):e68668.
[56] Conus S, Simon HU. Cathepsins and their involvement in immune responses. Swiss Med Weekly 2010;140:4–11. https://doi.org/10.4414/smw.2010.13042.
[57] Lv Z, Qiu L, Liu Z, Wang W, Chen H, Jia Y, et al. Molecular characterization of a cathepsin L1 highly expressed in phagocytes of pacific oyster *Crassostrea gigas*. Dev Comp Immunol 2018;89:152–62. https://doi.org/10.1016/j.dci.2018.08.014.
[58] Ford SE, Borrero FJ. Epizootiology and pathology of juvenile oyster disease in the eastern oyster, *Crassostrea virginica*. J Invertebr Pathol 2001;78(3):141–54. https://doi.org/10.1006/jipa.2001.5052.
[59] Paillard C. A short-review of brown ring disease, a vibriosis affecting clams, *Ruditapes philippinarum* and *Ruditapes decussatus*. Aquat Living Resour 2004;17 (4):467–75. https://doi.org/10.1051/alr:2004053.
[60] Walker JR, Ferrar PH. Diphenol oxidases, enzyme-catalysed browning and plant disease resistance. Biotechnol Genet Eng Rev 1998;15(1):457–98. https://doi.org/10.1080/02648725.1998.10647966.
[61] Allam B, Espinosa EP, Tanguy A, Jeffroy F, Le Bris C, Paillard C. Transcriptional changes in Manila clam (*Ruditapes philippinarum*) in response to Brown Ring Disease. Fish Shellfish Immunol 2014;41(1):2–11. https://doi.org/10.1016/j.fsi.2014.05.022.
[62] Cohen GM. Caspases: the executioners of apoptosis. Biochem J 1997;326 (1):1–16. https://doi.org/10.1042/bj3260001.
[63] Thornberry NA, Lazebnik Y. Caspases: enemies within. Science 1998;281 (5381):1312–6. https://doi.org/10.1126/science.281.5381.1312.
[64] Salvesen GS, Riedl SJ. Caspase mechanisms. Programmed Cell Death Cancer Progression Ther 2008:13–23. https://doi.org/10.1007/978-1-4020-6554-5_2.